Supplemental data

The Potentially Significant Role of CYP3A-Mediated Oxidative Metabolism of Dabigatran Etexilate and its Intermediate Metabolites in Drug-Drug Interaction Assessments Using Microdose Dabigatran Etexilate

Udomsak Udomnilobol, Suree Jianmongkol, Thomayant Prueksaritanont

Department of Pharmacology and Physiology, Faculty of Pharmaceutical Sciences, Chulalongkorn University, Bangkok, Thailand (U.U., S.J.).

Chulalongkorn University Drug Discovery and Drug Development Research Center (Chula4DR), Chulalongkorn University, Bangkok, Thailand (U.U., T.P.).

Supp. Table 1: BIBR0951 and its metabolites detected in the NADPH-fortified incubations.

Species	RT (min)	$[M+H]^+$ m/z (amu)	Structures	Product ion formula $[P]^+$ or $[P]^{\bullet+}$, m/z (amu)	Detected in*
M324	1.43	$[C_{17}H_{18}N_5O_2]^+$ 324.1461	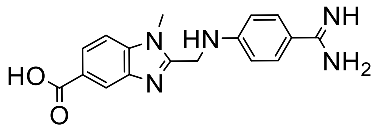	$[C_8H_7N_2]^+$, 131.0615; $[C_7H_8N_2O]^{\bullet+}$, 136.0626; $[C_8H_{10}N_3]^+$, 148.0874; $[C_{10}H_9N_2O_2]^+$, 189.0664; **$[C_{17}H_{13}N_4O]^+$, 289.1079**	HIM rhCYP3A4
M488	1.61	$[C_{25}H_{26}N_7O_4]^+$ 488.2044	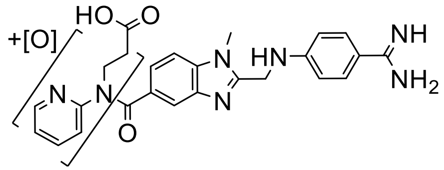	$[C_7H_8N_2O]^{\bullet+}$, 136.0626; $[C_8H_{10}N_3]^+$, 148.0867; $[C_8H_9N_2O_2]^+$, 165.0661; $[C_{10}H_8N_2O]^{\bullet+}$, 172.0651; $[C_{10}H_9N_2O_2]^+$, 189.0666; **$[C_{17}H_{13}N_4O]^+$, 289.1076**; $[C_{17}H_{16}N_5O]^+$, 306.1336; $[C_{17}H_{18}N_5O_2]^+$, 324.1461	HIM
DAB	1.81	$[C_{25}H_{26}N_7O_3]^+$ 472.2098	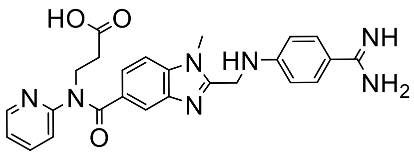	$[C_9H_9N_2]^+$, 145.0765; $[C_8H_{10}N_3]^+$, 148.0871; $[C_{10}H_8N_2O]^{\bullet+}$, 172.0641; $[C_{10}H_9N_2O_2]^+$, 189.0659; $[C_{15}H_{13}N_4O]^+$, 265.1090; $[C_{17}H_{13}N_4O]^+$, 289.1086; $[C_{17}H_{16}N_5O]^+$, 306.1348; $[C_{17}H_{18}N_5O_2]^+$, 324.1462; $[C_{18}H_{17}N_4O_3]^+$, 337.1303	HLM HIM rhCYP3A4 rhCYP3A5
M400	1.98	$[C_{22}H_{22}N_7O]^+$ 400.1889	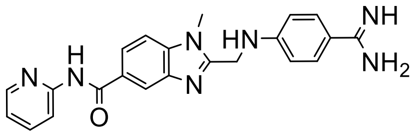	$[C_8H_7N_2]^+$, 131.0608; $[C_9H_8N_2]^{\bullet+}$, 144.0686; $[C_8H_{10}N_3]^+$, 148.0872; $[C_{10}H_8N_2O]^{\bullet+}$, 172.0636; $[C_{15}H_{12}N_4O]^{\bullet+}$, 264.1011; $[C_{15}H_{13}N_4O]^+$, 265.1085; **$[C_{17}H_{13}N_4O]^+$, 289.1086**; $[C_{22}H_{17}N_6]^+$, 365.1513; $[C_{22}H_{19}N_6O]^+$, 383.1618	HLM HIM rhCYP3A4 rhCYP3A5
M516 (1)	2.03	$[C_{27}H_{30}N_7O_4]^+$ 516.2377	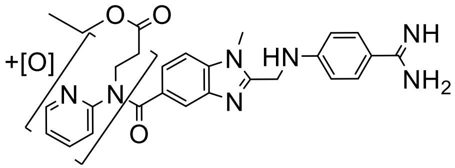	$[C_9H_9N_2]^+$, 145.0754; $[C_{10}H_8N_2O]^{\bullet+}$, 172.0628; $[C_{16}H_{17}N_5]^{\bullet+}$, 279.1482; **$[C_{17}H_{13}N_4O]^+$, 289.1081**; **$[C_{17}H_{16}N_5O]^+$, 306.1342**; $[C_{16}H_{17}N_5O_2]^{\bullet+}$, 311.1372; $[C_{18}H_{17}N_4O_3]^+$, 337.1671; $[C_{25}H_{26}N_7O_3]^+$, 472.2472	HLM HIM rhCYP3A4

M416	2.10	$[C_{22}H_{22}N_7O_2]^+$ 416.1834	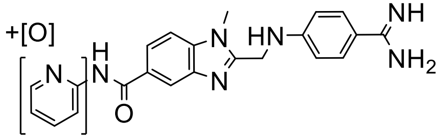	$[C_7H_8N_2O]^{\bullet+}$, 136.0621; $[C_9H_8N_2]^{\bullet+}$, 144.0697; $[C_9H_9N_2]^+$, 145.0769; $[C_{10}H_8N_2O]^{\bullet+}$, 172.0625; **$[C_{17}H_{13}N_4O]^+$, 289.1089**; $[C_{17}H_{16}N_5O]^+$, 306.1342	HIM rhCYP3A4
M516 (2)	2.16	$[C_{27}H_{30}N_7O_4]^+$ 516.2370	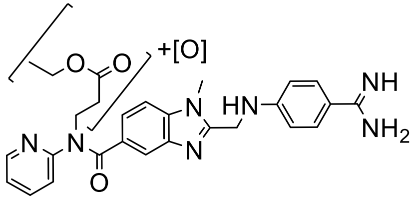	$[C_9H_9N_2]^+$, 145.0756; $[C_8H_9N_2O_2]^+$, 165.0661; $[C_{10}H_8N_2O]^{\bullet+}$, 172.0638; $[C_{10}H_9N_2O_2]^+$, 189.0659; **$[C_{10}H_{13}N_2O_2]^+$, 193.0978; $[C_{17}H_{13}N_4O]^+$, 289.1091**; **$[C_{17}H_{16}N_5O]^+$, 306.1351**; $[C_{17}H_{18}N_5O_2]^+$, 324.1456	HLM HIM rhCYP3A4 rhCYP3A5
BIBR0951 (parent)	2.45	$[C_{27}H_{30}N_7O_3]^+$ 500.2406	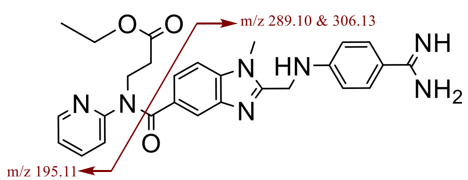	$[C_9H_8N_2]^{\bullet+}$, 144.0684; $[C_9H_9N_2]^+$, 145.0764; $[C_9H_7N_2O]^+$, 159.0556, $[C_{10}H_8N_2O]^{\bullet+}$, 172.0635; **$[C_{10}H_{15}N_2O_2]^+$, 195.1135**; $[C_{15}H_{12}N_4O]^{\bullet+}$, 264.1014; $[C_{16}H_{16}N_5]^+$, 278.1405; **$[C_{17}H_{13}N_4O]^+$, 289.1079**; **$[C_{17}H_{16}N_5O]^+$, 306.1349**; $[C_{22}H_{17}N_6]^+$, 365.1614	NA
M498 (1)	2.51	$[C_{27}H_{28}N_7O_3]^+$ 498.2257	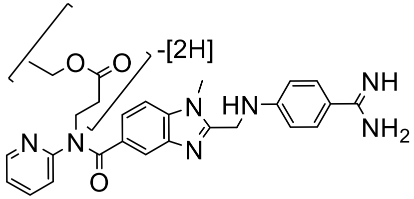	$[C_9H_8N_2]^{\bullet+}$, 144.0672; $[C_9H_9N_2]^+$, 145.0755; $[C_{10}H_8N_2O]^{\bullet+}$, 172.0639; $[C_{13}H_{15}N_3O_3]^{\bullet+}$, 261.1147; $[C_{16}H_{16}N_5]^+$, 278.1396; **$[C_{17}H_{13}N_4O]^+$, 289.1089**; **$[C_{17}H_{16}N_5O]^+$, 306.1351**; $[C_{13}H_{18}N_4O_3]^{\bullet+}$, 317.1034	HLM HIM rhCYP3A4 rhCYP3A5
M498 (2)	2.85	$[C_{27}H_{28}N_7O_3]^+$ 498.2261	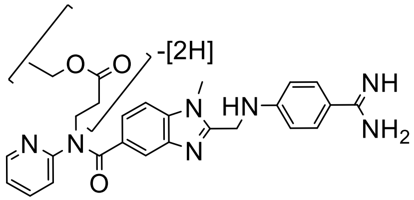	$[C_8H_7N_2]^+$, 131.0610; $[C_9H_9N_2]^+$, 145.0762; $[C_9H_7N_2O]^+$, 159.0562; $[C_{10}H_8N_2O]^{\bullet+}$, 172.0639; $[C_9H_8N_2O_2]^{\bullet+}$, 176.0583; **$[C_{17}H_{13}N_4O]^+$, 289.1086**; **$[C_{17}H_{16}N_5O]^+$, 306.1357**; $[C_{13}H_{18}N_4O_3]^{\bullet+}$, 317.1037; $[C_{25}H_{22}N_7O_2]^+$, 452.1841	HLM HIM rhCYP3A4

M514	3.35	$[C_{27}H_{28}N_7O_4]^+$ 514.2210	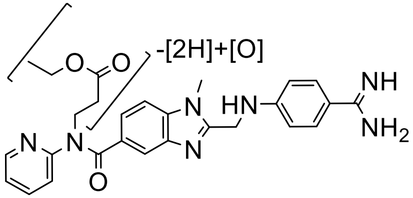	$[C_6H_7N_2O]^+$, 123.0565; $[C_7H_8N_2O]^{\bullet+}$, 136.0629; $[C_9H_9N_2]^+$, 145.0765, $[C_{10}H_8N_2O]^{\bullet+}$, 172.0644; **$[C_{17}H_{13}N_4O]^+$, 289.1106**; $[C_{17}H_{16}N_5O]^+$, 306.1360	HLM HIM rhCYP3A4

*The metabolites detected in the HLM and rhCYP3A4 incubations at 10 min, or in the HIM and rhCYP3A5 incubations at 60 min. RT, retention time; NA, not applicable.

Supp. Table 2: DABE and its metabolites detected in NADPH-fortified incubations.

Species	RT (min)	$[M+H]^+$ m/z (amu)	Structures	Product ion formula $[P]^+$ or $[P]^{\bullet+}$, m/z (amu)	Detected in*
DAB	1.82	$[C_{25}H_{26}N_7O_3]^+$ 472.2094	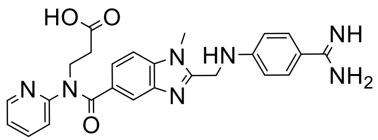	$[C_7H_8N_2O]^{\bullet+}$, 136.0619; $[C_9H_9N_2]^+$, 145.0758; $[C_{10}H_8N_2O]^{\bullet+}$, 172.0638; $[C_{17}H_{13}N_4O]^+$, 289.1092; $[C_{17}H_{16}N_5O]^+$, 306.1358; $[C_{17}H_{18}N_5O_2]^+$, 324.1452; $[C_{18}H_{17}N_4O_3]^+$, 337.1299; $[C_{22}H_{22}N_7O]^+$, 400.1852	HLM HIM rhCYP3A4
M400	2.00	$[C_{22}H_{22}N_7O]^+$ 400.1891	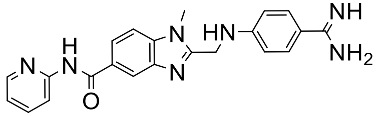	$[C_8H_7N_2]^+$, 131.0607; $[C_7H_8N_2O]^{\bullet+}$, 136.0622; $[C_8H_{10}N_3]^+$, 148.0873; $[C_{10}H_8N_2O]^{\bullet+}$, 172.0637; $[C_{15}H_{12}N_4O]^{\bullet+}$, 264.1008; $[C_{15}H_{13}N_4O]^+$, 265.1091; **$[C_{17}H_{13}N_4O]^+$, 289.1087**; $[C_{22}H_{17}N_6]^+$, 365.1511; $[C_{22}H_{19}N_6O]^+$, 383.1621	HLM HIM
BIBR0951	2.47	$[C_{27}H_{30}N_7O_3]^+$ 500.2411	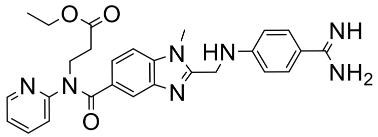	$[C_9H_9N_2]^+$, 145.0764; $[C_9H_7N_2O]^+$, 159.0563; $[C_{10}H_8N_2O]^{\bullet+}$, 172.0637; $[C_{13}H_{15}N_3O_3]^+$, 261.1129; $[C_{15}H_{12}N_4O]^{\bullet+}$, 264.0977; $[C_{17}H_{13}N_4O]^+$, 289.1090; $[C_{17}H_{16}N_5O]^+$, 306.1354; $[C_{22}H_{17}N_6]^+$, 365.1636	HLM HIM rhCYP3A4 rhCYP3A5
M644 (1)	3.05	$[C_{34}H_{42}N_7O_6]^+$ 644.3201	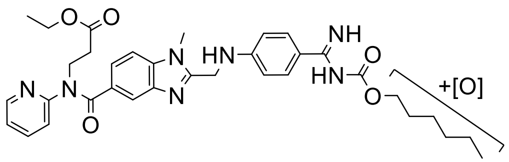	$[C_{10}H_8N_2O]^{\bullet+}$, 172.0617; **$[C_{17}H_{13}N_4O]^+$, 289.1084**; $[C_{17}H_{16}N_5O]^+$, 306.1375; $[C_{18}H_{14}N_5O_2]^+$, 332.1149; $[C_{27}H_{30}N_7O_3]^+$, 500.2356; **$[C_{28}H_{28}N_7O_4]^+$, 526.2182**	HLM HIM rhCYP3A4 rhCYP3A5
M644 (2)	3.11	$[C_{34}H_{42}N_7O_6]^+$ 644.3207	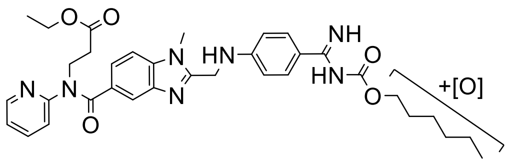	$[C_{17}H_{13}N_4O]^+$, 289.1079; **$[C_{15}H_{19}N_3O_3]^{\bullet+}$, 289.1087**; $[C_{17}H_{16}N_5O]^+$, 306.1327; $[C_{18}H_{14}N_5O_2]^+$, 332.1152; $[C_{27}H_{28}N_6O_4]^{\bullet+}$, 500.2188; $[C_{27}H_{30}N_7O_3]^+$, 500.2414; **$[C_{28}H_{28}N_7O_4]^+$, 526.2192**	HLM HIM rhCYP3A4 rhCYP3A5

M264	3.28	$[C_{14}H_{22}N_3O_2]^+$ 264.1707	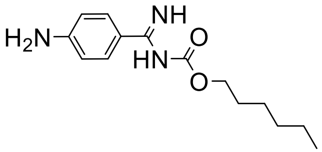	$[C_6H_6N]^+$, 92.0501; $[C_7H_7N_2]^+$, 119.0608; $[C_7H_{10}N_3]^+$, 136.0872; $[C_8H_8N_3O]^+$, 162.0673; $[C_8H_{10}N_3O_2]^+$, 180.0775	HLM HIM rhCYP3A4 rhCYP3A5
BIBR1087	3.39	$[C_{32}H_{38}N_7O_5]^+$ 600.2928	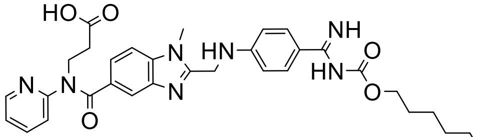	$[C_8H_9N_2O]^+$, 149.0715; $[C_{17}H_{13}N_4O]^+$, 289.1089; $[C_{17}H_{16}N_5O]^+$, 306.1354; $[C_{18}H_{14}N_5O_2]^+$, 332.1150; $[C_{18}H_{16}N_5O_3]^+$, 350.1250; $[C_{24}H_{28}N_5O_3]^+$, 434.2193; $[C_{25}H_{24}N_7O_2]^+$, 454.1993	HLM HIM rhCYP3A4 rhCYP3A5
M528	3.64	$[C_{29}H_{34}N_7O_3]^+$ 528.2727	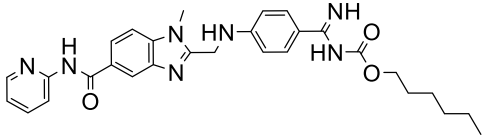	$[C_8H_{10}N_3]^+$, 148.0871; $[C_{15}H_{13}N_4O]^+$, 265.1103; **$[C_{17}H_{13}N_4O]^+$, 289.1096**; $[C_{17}H_{16}N_5O]^+$, 306.1361; $[C_{22}H_{17}N_6]^+$, 365.1508; $[C_{22}H_{19}N_6O]^+$, 383.1623; $[C_{22}H_{22}N_7O]^+$, 400.1887; **$[C_{23}H_{20}N_7O_2]^+$, 426.1675**	HLM HIM rhCYP3A4 rhCYP3A5
DABE (parent)	3.95	$[C_{34}H_{42}N_7O_5]^+$ 628.3240	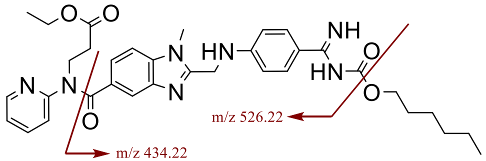	$[C_{10}H_8N_2O]^{\bullet+}$, 172.0638; $[C_{10}H_9N_2O_2]^+$, 189.0667; **$[C_{17}H_{13}N_4O]^+$, 289.1091**; $[C_{17}H_{16}N_5O]^+$, 306.1359; $[C_{18}H_{14}N_5O_2]^+$, 332.1149; $[C_{22}H_{17}N_6]^+$, 365.1613; **$[C_{24}H_{28}N_5O_3]^+$, 434.2194**; **$[C_{28}H_{28}N_7O_4]^+$, 526.2194**	NA

*The metabolites detected in the HLM, HIM, rhCYP3A4, and rhCYP3A5 incubations at 10 min. RT, retention time; NA, not applicable.

Supp. Table 3: Formation kinetic of primary metabolites following incubation of either DABE or BIBR0951 in NADPH-fortified rhCYP3A4 and rhCYP3A5.

Metabolic reactions	rhCYP3A4			rhCYP3A5		
	V_{max} (pmol/min/pmol)	K_m (µM)	CL_{int} (µL/min/pmol)	V_{max} (pmol/min/pmol)	K_m (µM)	CL_{int} (µL/min/pmol)
DABE						
BIBR0951 formation	ND	ND	ND	ND	ND	ND
M644 (1) and (2) formation	NA	0.6 ± 0.1	NA	NA	0.6 ± 0.04	NA
M264 formation	NA	0.3 ± 0.1	NA	NA	0.3 ± 0.1	NA
BIBR1087 formation	2.7 ± 0.1	0.4 ± 0.04	7.2 ± 0.5	1.4 ± 0.1	0.6 ± 0.1	2.4 ± 0.5
M528 formation	NA	1.4 ± 0.3	NA	NA	2.4 ± 0.2	NA
BIBR0951						
DAB formation	2.6 ± 0.2	3.7 ± 0.5	0.7 ± 0.1	0.9 ± 0.03	2.8 ± 0.3	0.3 ± 0.03
M400 formation	NA	2.9 ± 0.1	NA	NA	1.2 ± 0.1	NA
M516 (1) formation	NA	3.7 ± 0.3	NA	NA	NA	NA
M516 (2) formation	NA	2.8 ± 0.3	NA	NA	1.6 ± 0.4	NA
M498 (1) formation	NA	4.6 ± 0.3	NA	NA	1.1 ± 0.1	NA
M498 (2) formation	NA	3.1 ± 0.3	NA	NA	NA	NA

Data are expressed as mean ± SD from n=3. NA, not applicable due to lack of analytical standards. ND, no data due to negligible metabolite formation.

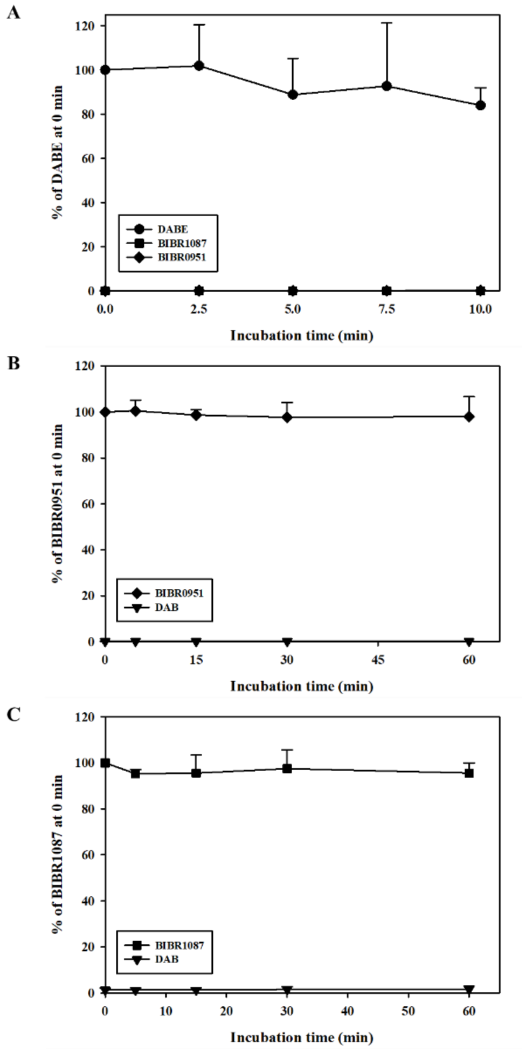

Supp. Figure 1: Stability of DABE (A), BIBR0951 (B), and BIBR1087 (C) in the phosphate buffer fortified with NADPH (no microsomal protein). Data are expressed as mean ± SD from n=3.

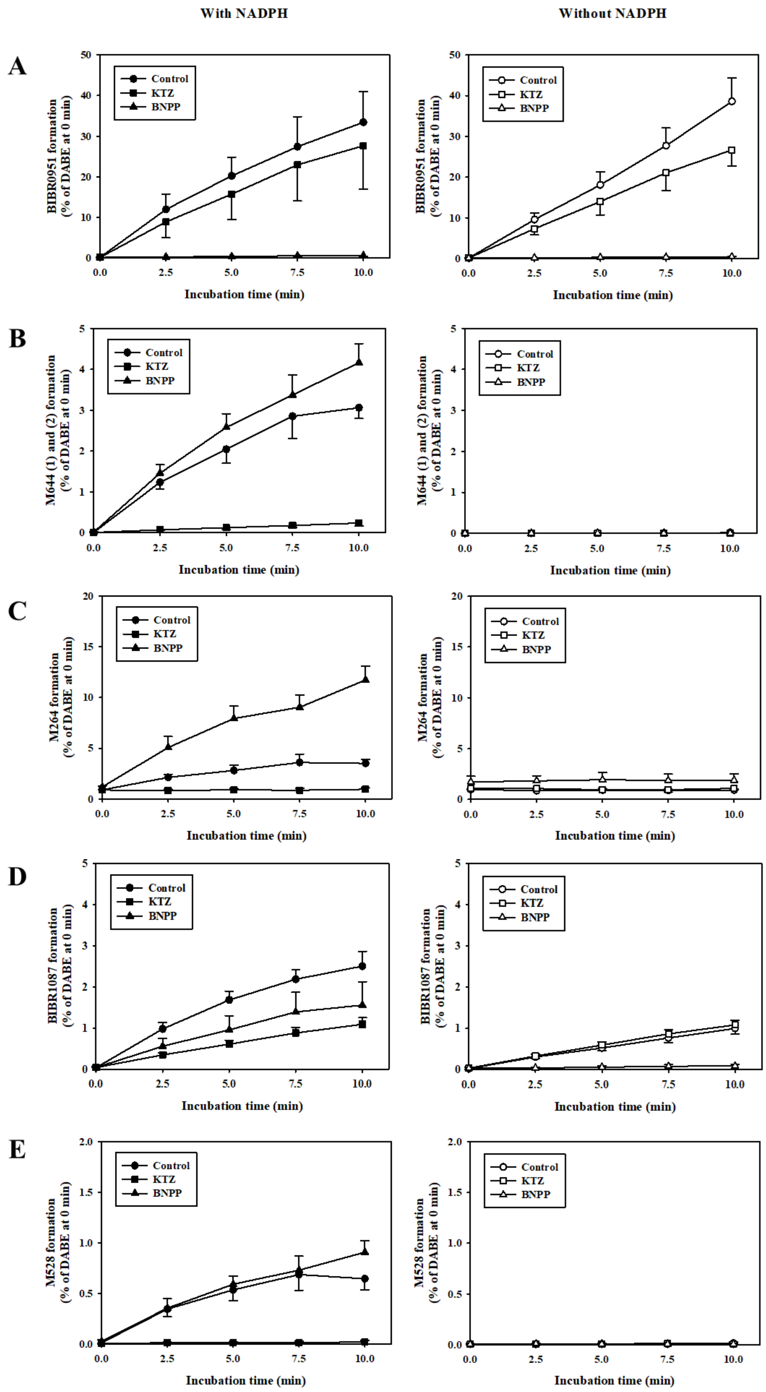

Supp. Figure 2: Effects of KTZ (1 µM) and BNPP (100 µM) on the formation of BIBR0951 (A), M644 (1) and (2) (B), M264 (C), BIBR1087 (D), and M528 (E) following incubation of 1 µM DABE in HIM with (left panel) or without (right panel) NADPH. Data are expressed as mean ± SD from n=3. The formation of M644 (1) and (2) was combined due to incomplete separation of chromatographic peaks.

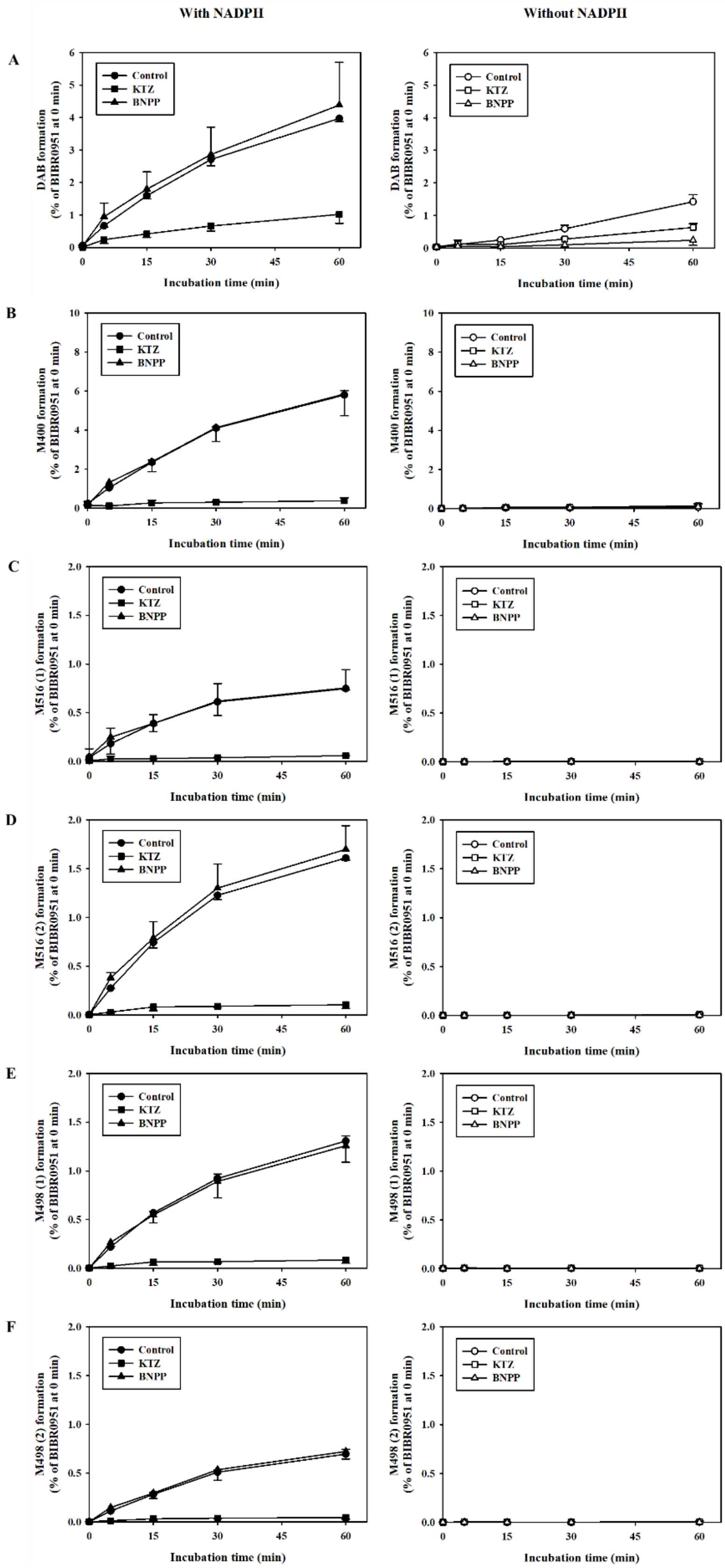

Supp. Figure 3: Effects of KTZ (1 µM) and BNPP (100 µM) on the formation of DAB (A), M400 (B), M516 (1) (C), M516 (2) (D), M498 (1) (E), and M498 (2) (F) following incubation of 1 µM BIBR0951 in HIM with (left panel) or without (right panel) NADPH. Data are expressed as mean ± SD from n=3.

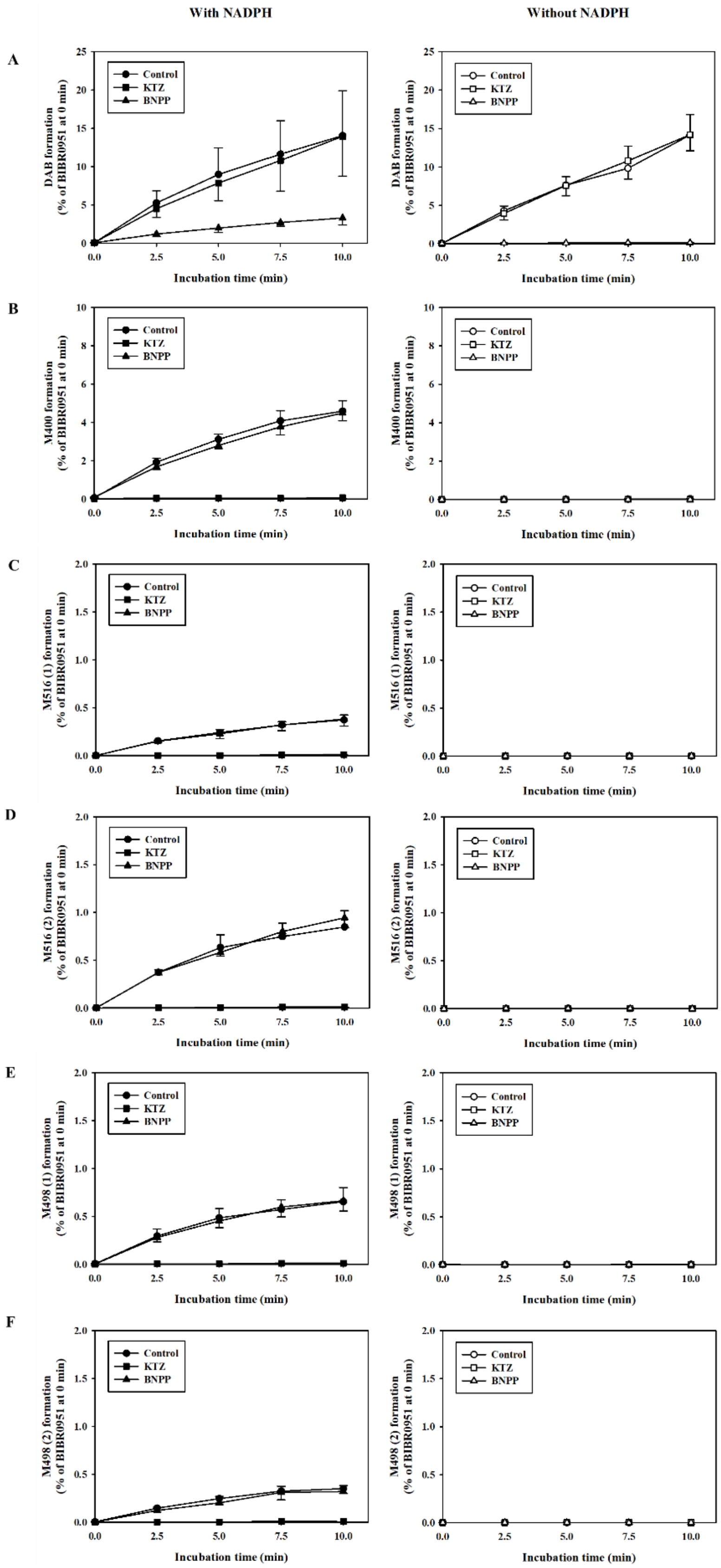

Supp. Figure 4: Effects of KTZ (1 µM) and BNPP (100 µM) on the formation of DAB (A), M400 (B), M516 (1) (C), M516 (2) (D), M498 (1) (E), and M498 (2) (F) following incubation of 1 µM BIBR0951 in HLM with (left panel) or without (right panel) NADPH. Data are expressed as mean ± SD from n=3.

A

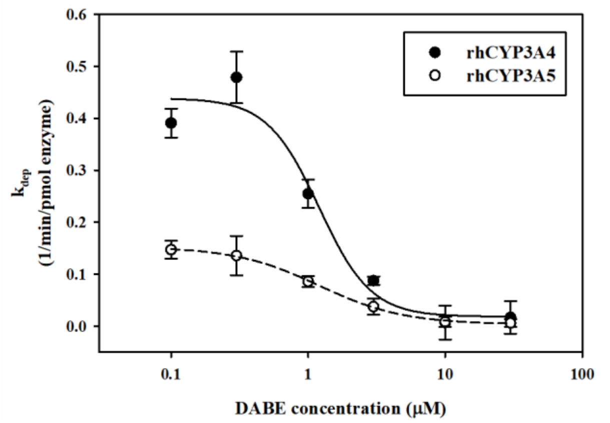

B

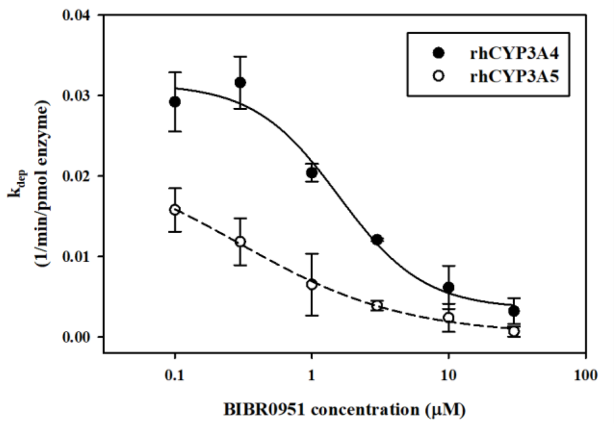

Supp. Figure 5: Plots of *in vitro* depletion rate constants (k_{dep}) of DABE (A) and BIBR0951 (B) versus concentrations in the NADPH-fortified rhCYP3A4 and rhCYP3A5 systems. Data are expressed as mean ± SD from n=3.

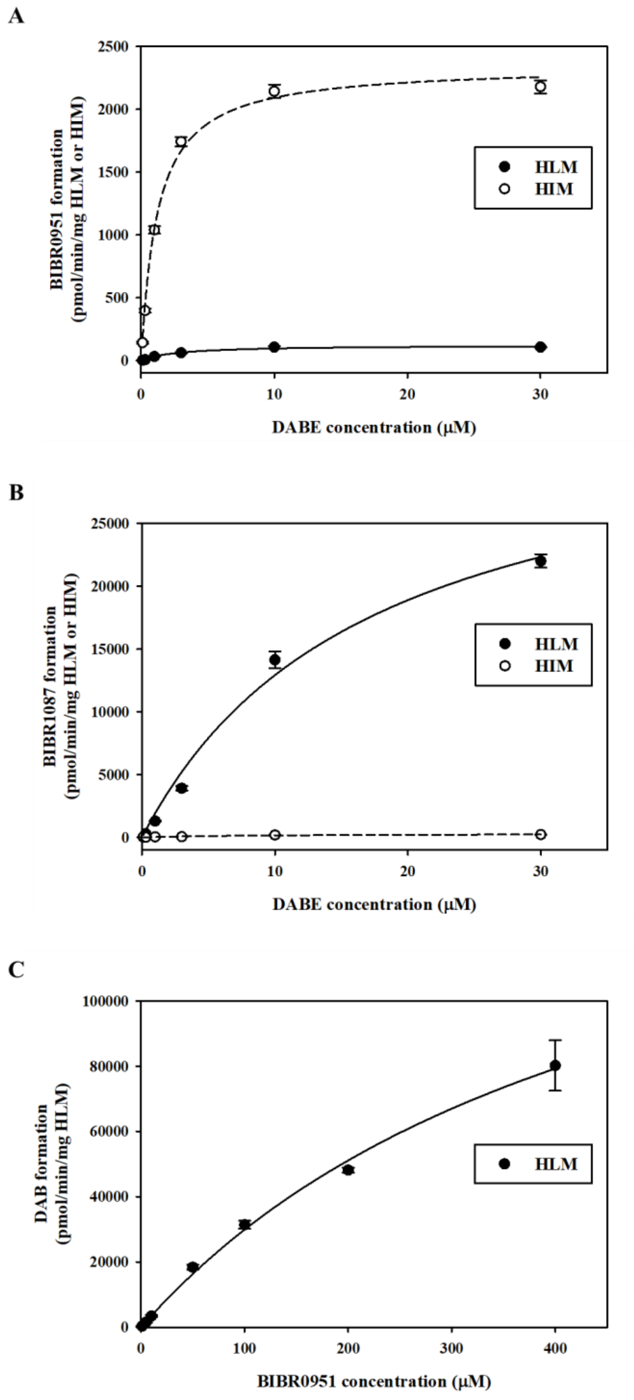

Supp. Figure 6: Michaelis-Menten kinetics of CES-mediated hydrolysis of DABE (A and B) and BIBR0951 (C) in HLM and HIM. Data are expressed as mean ± SD from n=3. The DAB formation was negligible in the HIM incubation with BIBR0951.

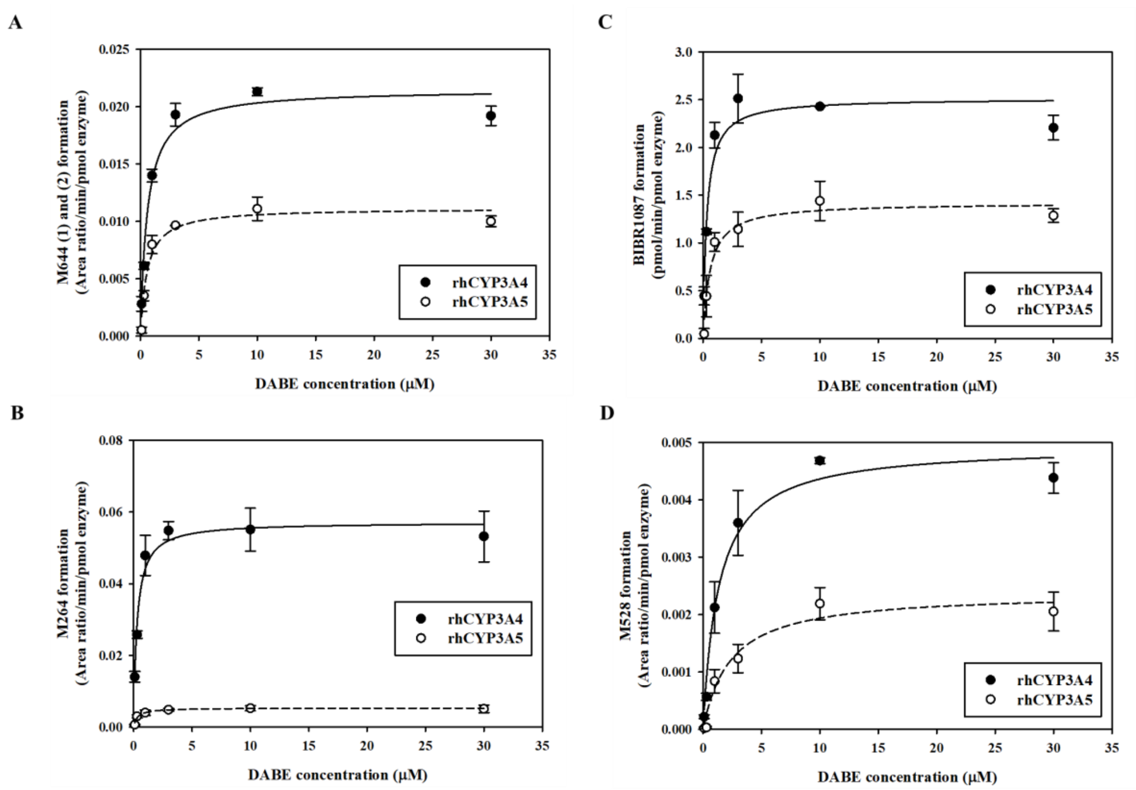

Supp. Figure 7: The formation of M644 (1) and (2) (A), M264 (B), BIBR1087 (C), and M528 (D) following incubation of DABE in NADPH-fortified rhCYP3A4 and rhCYP3A5 systems. Data are expressed as mean ± SD from n=3. The formation of M644 (1) and (2) was combined due to incomplete separation of chromatographic peaks.

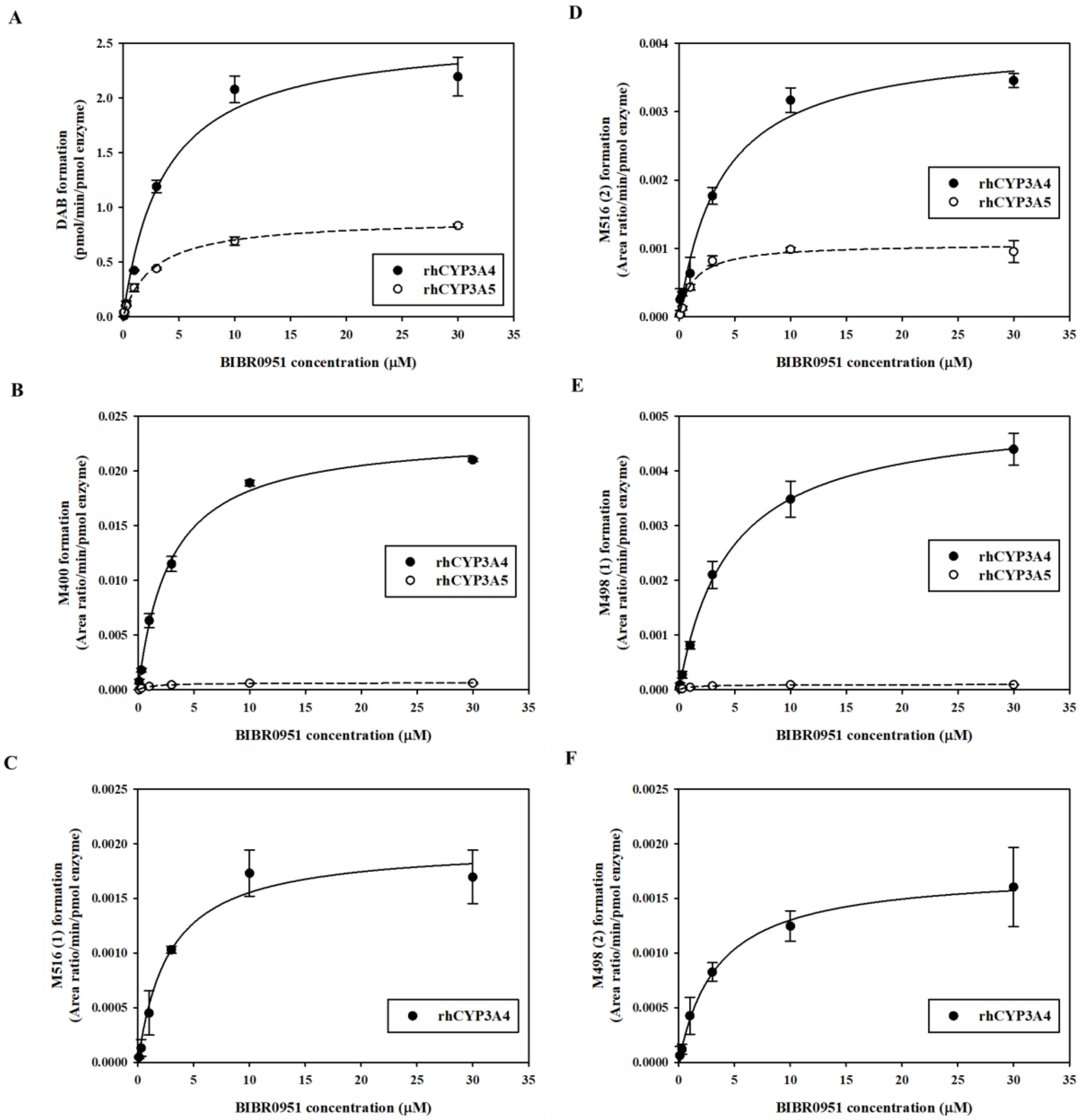

Supp. Figure 8: The formation of DAB (A), M400 (B), M516 (1) (C), M516 (2) (D), M498 (1) (E), and M498 (2) (F) following incubation of BIBR0951 in NADPH-fortified rhCYP3A4 and rhCYP3A5 systems. Data are expressed as mean ± SD from n=3. M516 (1) and M498 (2) were not formed in the rhCYP3A5 system.

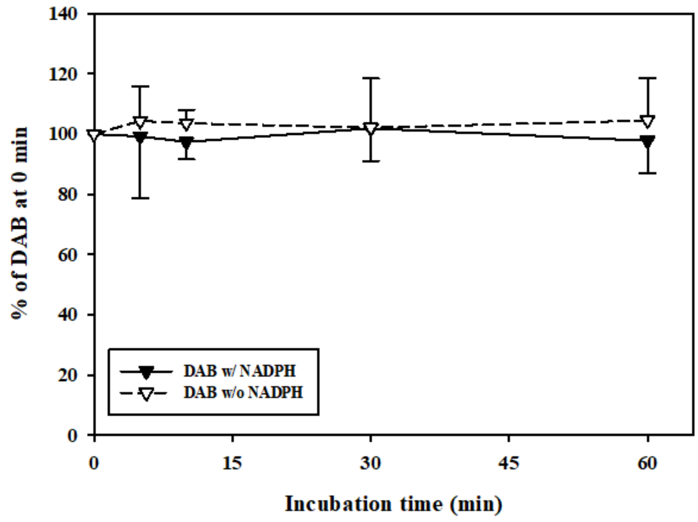

Supp. Figure 9: Metabolic stability of DAB (1 µM) in HLM (0.5 mg/mL). Black symbols and solid lines represent the incubations with NADPH, whereas white symbols and dashed lines represent the incubations without NADPH. Data are expressed as % of DAB compared to 0 min (mean ± SD from n = 3).